The Egyptian Journal of Remote Sensing and Space Sciences 21 (2018) S13–S22

HOSTED BY

ELSEVIER

Contents lists available at ScienceDirect

The Egyptian Journal of Remote Sensing and Space Sciences

journal homepage: www.sciencedirect.com

Research Paper

Soil moisture estimation in Ferlo region (Senegal) using radar (ENVISAT/ASAR) and optical (SPOT/VEGETATION) data

Gayane Faye [a,*], Pierre-Louis Frison [d], Abdou-Aziz Diouf [b], Souleye Wade [a], Cheikh Amidou Kane [c], Fabio Fussi [e], Lionel Jarlan [f], Magatte Fary Kani Niang [a], Jacques André Ndione [b], Jean Paul Rudant [d], Eric Mougin [g]

[a] *Laboratoire de Télédétection Appliquée – Institut des Sciences de la Terre – Université Cheikh Anta Diop, BP 5396 Dakar-Fann, Senegal*
[b] *Centre de Suivi Ecologique (CSE), rue Léon Gontran Damas, BP 15532 Dakar-Fann, Senegal*
[c] *Université de Thies, Senegal*
[d] *Université Paris-Est, IGN, LaSTIG//MATIS, 6-8 av. B. Pascal, Cité Descartes, Champs sur Marne, 77455 Marne la Vallée Cedex 2, France*
[e] *Fabio FUSSI, Milano BICCOCA University, Milano, Italy*
[f] *CESBIO, 18 avenue, Édouard Belin, bp 2801, 31401 Toulouse cedex 9, France*
[g] *Géosciences Environnement Toulouse, UMR 5563, France*

ARTICLE INFO

Article history:
Received 21 March 2017
Revised 30 October 2017
Accepted 20 November 2017
Available online 1 December 2017

Keywords:
Soil moisture
Radar remote sensing
ASAR
ERS
SPOT-VEGETATION
Ferlo

ABSTRACT

The sensitivity of the radar signal to the seasonal dynamics in the Sahel region is a considerable asset for monitoring surface parameters including soil moisture. Given the sensitivity of the radar signal to vegetation mass production, roughness and soil moisture, the main problem has been to estimate the contribution of these three parameters to the signal. This study aims to circumvent this problem by combining radar with optical data. The DMP (Dry Mater Product) extracted from SPOT data allowed to estimate vegetation mass production. Surface roughness was estimated from radar data during the dry season. Because during the dry season, radar signal is only conditioned by soil roughness in this region a Radiative Transfer Model (RTM) was used: it consists in a microwave scattering model of layered vegetation based on the first-order solution of the radiative transfer equation and it accounts for multiple scattering within the canopy, surface roughness of the soil, and the interaction between canopy surface and soil.

This model was designed to account for the branch size distribution, leaf orientation distribution, and branch orientation distribution for each size. In this study, the RTM has been calibrated with ESCAT (European Radar Satellite Scatterometer) data, and has been used in order to estimate soil moisture.

The results obtained have allowed to track the spatial and temporal dynamics of soil moisture on the one hand, and on the other hand the influence of geology and morphopedology on the spatial dynamics of the soil moisture variability. These results are promising despite the fact that the inversed RTM often faces difficulties to interpret the signal for saturated soils, giving an aberrant value of soil moisture more often than not.

1. Introduction

Estimating and monitoring the spatial and temporal evolution of soil moisture is of paramount importance in many areas. They allow among other things, better monitoring of crops and agricultural yields. Radar remote sensing offers strong potential for applications, due to its sensitivity to the dynamics of continental surfaces. Indeed, some studies have underlined the strong seasonal dependence of the radar signal in semi-arid zones, especially in the Sahel, which makes it possible to discriminate the alternative dry and wet seasons (Baup et al., 2007; Dubois et al., 1995; Faye

Peer review under responsibility of National Authority for Remote Sensing and Space Sciences.

* Corresponding author.
E-mail addresses: gayane.faye@gmail.com (G. Faye), pierre-louis.frison@u-pem.fr (P.-L. Frison), aziz.diouf@cse.sn (A.-A. Diouf), wadesouleye@yahoo.fr (S. Wade), kachakane@yahoo.fr (C.A. Kane), fabio.fussi@usa.net (F. Fussi), lionel.jarlan@ird.fr (L. Jarlan), magniang@refer.sn (M.F.K. Niang), jacques-andre.ndione@cse.sn (J.A. Ndione), Jean-Paul.Rudant@u-pem.fr (J.P. Rudant), eric.mougin@get.obs-mip.fr (E. Mougin).

https://doi.org/10.1016/j.ejrs.2017.11.005
1110-9823/

et al., 2011; Frison and Mougin, 1996a,b; Frison et al., 1998; Jarlan et al., 2003; Le Toan et al., 1981; Magagi and Kerr, 1997; Naeimi et al., 2009; Pellarin et al., 2006; Wagner et al., 1999, 2000; Woodhouse and Hoekman, 2000; Zine et al., 2005; Zribi and Dechambre, 2002). In the Sahel region, the radar signal is sensitive to land surface parameters: vegetation mass production, roughness and soil moisture (Ulaby et al., 1978; Bernard et al., 1981; Bradley and Ulaby 1981; Bruckler et al., 1988; Dobson and Ulaby 1986; Naeimi et al., 2009). Globally radar sensors have demonstrated their potential for the effective measurement and monitoring of soil surface characteristics (Baghdadi et al., 2008; Rahman et al., 2008; Thoma et al., 2008; Anguela et al., 2010; Pandey and Pandey 2010; Aubert et al., 2011; Zribi et al., 2011; Molin and Faulin, 2013; Castaldi et al., 2014; Gorrab et al., 2015).

In fact the temporal evolution of the radar signal is strongly correlated with the increase in soil moisture and the development of vegetation (Faye et al., 2011; Zine et al., 2005; Zribi and Dechambre, 2002). In the past two decades some studies have aimed to estimate soil moisture from radar remote sensing data, (Baghdadi et al., 2012; Castaldi et al., 2014; Wagner et al., 2000) and data acquired with Synthetic Aperture Radar (SAR) yielded fairly consistent results (Zribi and Dechambre, 2002; Zribi et al., 2014).

The purpose of this work was to estimate soil moisture in semi-arid areas of Senegal by using the ENVISAT ASAR (Advanced Synthetic Aperture Radar) data and a Radiative Transfer Model (RTM), which is a backscattering model based on the first-order solution of the radiative transfer equation (Karam et al., 1992). However, considering the dependence of the radar signal on the three surface parameters (soil moisture, surface roughness and biomass) the main difficulty encountered was how to determine the singular contribution of each parameter to the radar response.

For this reason, we calculated soil roughness from dry season radar data and vegetation mass from the Dry Mater Productivity (DMP) product derived from the SPOT VEGETATION-2 optical sensor data on SPOT-5 satellite (Bégué, 2002; Kumar and Monteith, 1981; Varlet-Grancher et al., 1982; ftp. www.vito-eodata.be/).

2. Data and methods

2.1. Study areas

The study area was in Senegal, covering the Sylvo-Pastoral zone of the Ferlo region and the northern groundnut basin. It expands to the coastal fringe (Fig. 1). The western part of the study area, which covers a large part of the coastal fringe, is characterized by a shallow aquifer, fairly extensive tree/shrub vegetation over a sandy soil, while the eastern part lays in the Ferlo region (Fig. 1) and is characterized by a water table that reaches up to 100 m deep. The annual rainfall is estimated to be between 200 and 500 mm, with a high inter-annual variability.

The western area and a large part of half of the northern area are dominated by a shrub steppe with sparse trees. Rainfed agriculture occupies the western and southern part of the study area, whereas irrigated crops dominate in the northwest, along with some marshy meadows. The southeast with a shrub savannah is a pasture zone.

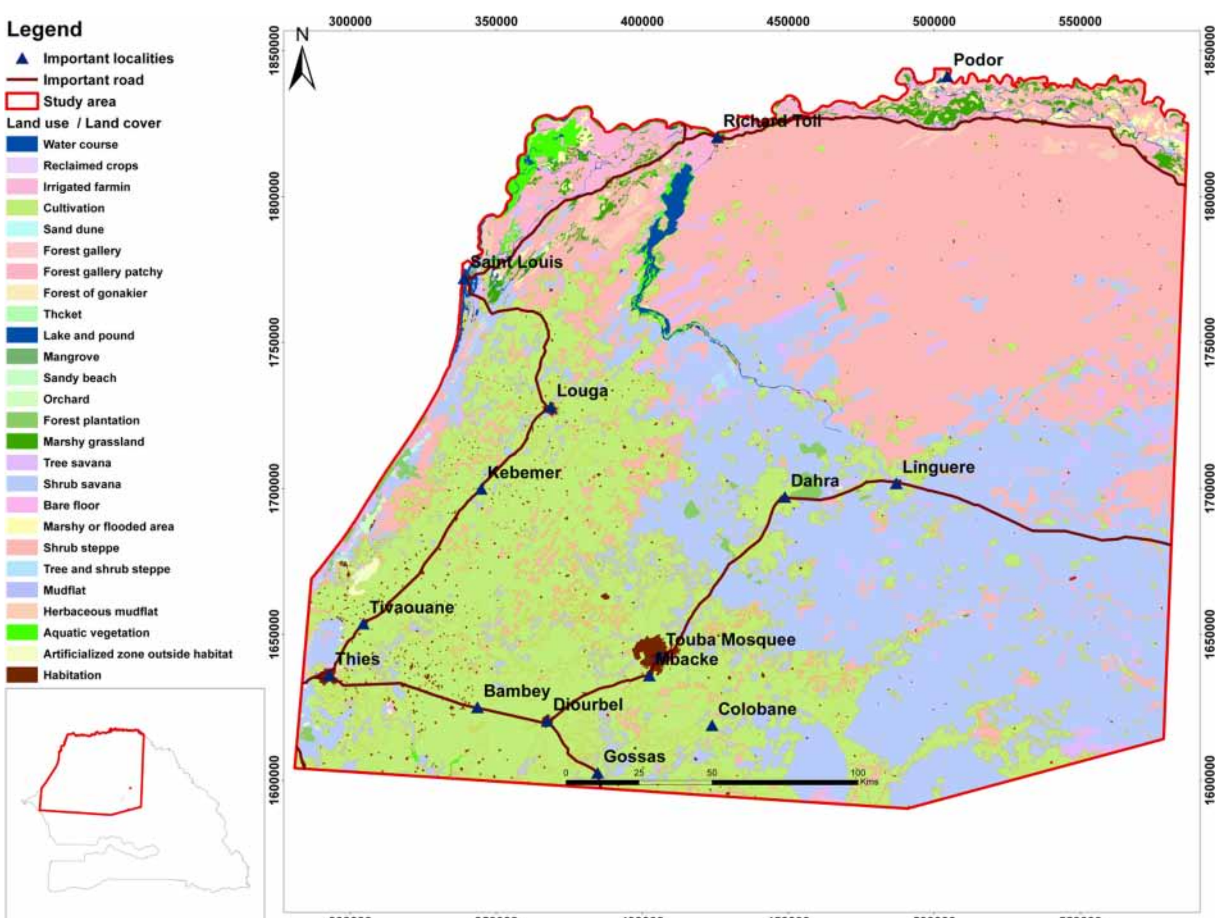

Fig. 1. Land use, land cover of the study area (PNAT, 1986).

The geological formations that condition the type of soil whose moisture is studied are presented here. These are alluvial or beach sands along the western coast, continental sand dunes in the center and north and silty sands with outcrops of limestone, marl and kaolinic clay in the East (Fig. 2, Table 1, PNAT, 1986).

The area includes sand dune formations that are generally poorly developed or degraded Sahelian domain soils. These are tropical ferruginous soils in the south, alternating with brown red soils in the north. Hydromorphic soils are found along the valleys. In the East, there are subaridal brown soils, lithosols and poorly developed soils. Some mudflats develop in the north-eastern part, in the vicinity of the delta (PNAT, 1986).

2.2. Data description

Two types of data sets were used: remote sensing data and field measurements for calibrating the Radiative Transfer Model.

2.2.1. Field data

The *in situ* vegetation mass measurements were collected from the *Centre de Suivi Ecologique* (CSE) database. Indeed, at the end of the rainy season, during peak vegetation levels, the CSE conducts field measurements of herbaceous production (www.cse.sn, Diouf et al., 1998). These measurements make it possible to determine the amplitude of the temporal simulations of the vegetation from the Sahelian Transpiration Evaporation and Production model (STEP; Mougin et al., 1995). Rainfall measurements from the National Agency for Civil Aviation and Meteorology ANACIM (*Agence Nationale de l'Aviation Civile et de la Météorologie*) are also used. In this study, we used daily rainfall data of Linguere station, which is the only station that measures all climate data (temperature, rainfall, etc.) in the study area.

2.2.2. Radar data

Two radar data sets, both acquired at C band, were analyzed: data acquired by the scatterometer (ESCAT) onboard ERS-1/2 (European Radar Satellite), and other data acquired by ASAR onboard ENVISAT that are highly sensitive to surface parameters dynamics, mainly soil moisture and crop production.

To calibrate the model, series of long-term observations through ESCAT (1992–2007) were used. Considering the need for the finest resolution possible and higher temporal repeatability, the ENVISAT-ASAR sensor data (2008–2011) from a 101-min revolution period with a 35-day orbital cycle were used. It provides HH and VV polarization images with a spatial resolution of 1 km. On average, 2–3 images in VV polarization are obtained per month in the study area.

2.2.3. Optical data

The DMP extracted from SPOT-VEGETATION data by the Flemish Institute for Technological Research (VITO; ftp. www.vito-eodata.be/), was used to estimate total vegetation mass production. In fact, the VEGETATION-2 sensor on board the SPOT-5 is an imaging system operating in the 4 spectral bands (Red, Green, Blue and Near Infrared) with a spatial resolution of about 1 km and a daily repeatability.

The DMP is an indicator that reflects daily increase in dry plant biomass. It is calculated from NDVI and meteorological data such as global solar radiation and temperature provided by ECMWF (European Centre for Medium-Range Weather Forecasts; Bégué, 2002; Kumar and Monteith 1981; Varlet-Grancher et al. 1982).

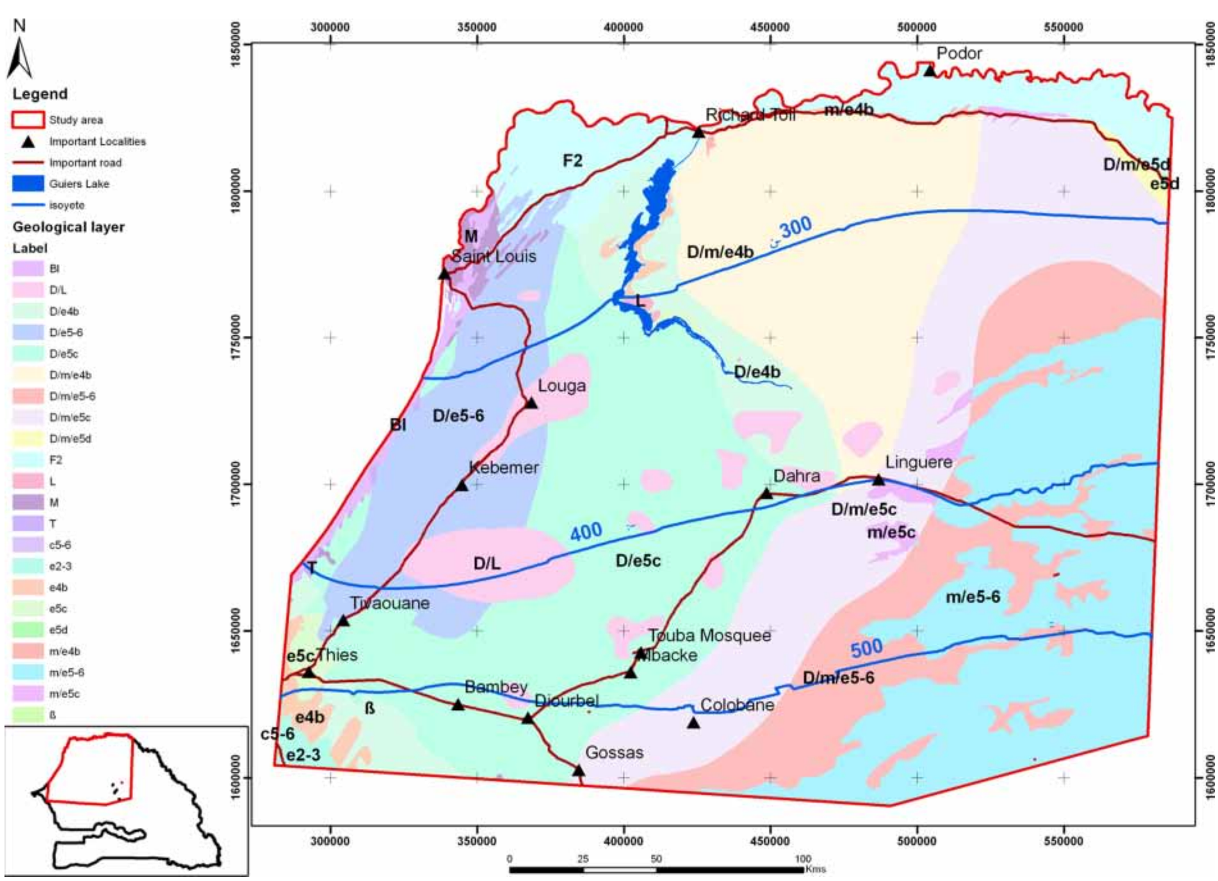

Fig. 2. Localization and geological map of the study area (PNAT, 1986).

Table 1
Codification of geological layers in the study area.

Geological layers	Code
Recent fluviatile Alluvium	F2
Beach sands and dune seams: coastal barrier	Bl
Shellfish vase and sand of slikkes, schorres and interdistributary lagoons	M
Interdunary humus sand, locally peaty, shelly: black soil of the Niayes	T
Rubified sand of continental dunes/White clay and marls with attapulgite and silicate phosphate-glauconic horizons	D/e4b
Rubified sand of continental dunes/Limestones and marls with nummilites, phosphate in the west	D/e5–6
Rubified sand of continental dunes/Alternations of marls with discocyclines and yellow limestone with molluscs, sea urchins and algaes	D/e5c
Rubified sand of continental dunes/Lacastrine limestone	D/L
Rubified sand from of continental dunes/Bioturbated sandstone and kaolinic clays for burrows and molluscs/White clays and marls with attapulgite and silicate phosphate-glauconic horizons	D/m/e4b
Rubified sand of continental dunes/Bioturbated sandstone and kaolinic clays with burrows and molluscs/Limestones and marls with phosphate nummilites in the west	D/m/e5–6
Rubified sand of continental dunes/Bioturbated and kaolinic clays with burrows and molluscs/Alternations of marls with discocyclines and yellow limestones with molluscs, sea urchins and algae	D/m/e5c
Rubified sand from continental dunes/Bioturbated sandstones and kaolinic clays for burrows and molluscs/Limestones, marls and ocher-yellow clay with attapulgite, fossiliferous and phosphate horizon	D/m/e5d
Shellfish limestone with molluscs	e2–3
Lacustre limestone	L
Limestones, marls and ocher-yellow clays with attapulgite, fossiliferous and phosphate horizons	e5d
Alternations of marls with discocyclines and yellow limestone with molluscs, sea urchins and algae	e5c
Clays and white marls with attapulgite and silicate phosphate-glauconic horizons	e4b
Bioturbated sandstones and kaolinite clays for burrows and molluscs/White clay and marls with attapulgite and silicate phosphate-glauconic horizons	m/e4b
Bioturbated sandstones and kaolinic clays for burrows and molluscs/Limestones and marls with nummulites; phosphaties to the west	m/e5–6
Bioturbated sandstones and kaolonic clays for burrows and molluscs/Alternations of discocycline marls and yellow limestone with molluscs, sea urchins and algae	m/e5c
Sandstones and clays	c5–6
Tertiary and quaternary volcanic products (dolerites, basanites, basalts, tuff)	Beta

The DMP products have a spatial resolution of 1 km and a decadal time step. They represent the average daily productivity for each decade. To obtain the total vegetation mass productivity of each decade, it is necessary to multiply by ten. Then total vegetation mass available for a given decade is calculated by adding the decadal vegetation mass productivity, the beginning of rainy season being fixed in the first decade of June.

2.3. Methodology

In Sahelian zone, the radar signal in C band depends mainly on three parameters: soil moisture, surface roughness and vegetation mass (Frison et al., 1998; Jarlan et al., 2002; Zine et al., 2005). Knowing two of these parameters makes it possible to estimate the third one. The Radiative Transfer Model (RTM) is an electromagnetic model which enables us to simulate the interaction of an electromagnetic wave with a terrestrial surface (Karam et al., 1992). It allows the simulation of the radar signal from the surface parameters (vegetation cover, roughness, dielectric constant which is highly dependent on soil moisture). Consequently, the influence of the vegetation cover and soil parameters (roughness, dielectric constant) can be analyzed. The input data of the model are plant production, soil roughness and soil moisture.

The results of these simulations were then compared with the measured radar signal for proper calibration of the model (we named this step: direct model). This model has been validated in two semi-arid zones of the Sahel (Frison et al., 1998; Jarlan et al., 2002; Zine et al., 2005). These authors have shown that, from a knowledge of surface parameters over Sahelian regions, the measured radar signal can be reconstructed.

Given the lack of *in situ* data at a daily rate, the Sahelian Transpiration Evaporation and Production (STEP) model, (Mougin et al., 1995), describing the temporal evolution of the scene was used to simulate daily vegetation mass and soil moisture to calibrate RTM. STEP is a relatively simple ecosystem model which describes the relevant processes of soil-vegetation atmosphere system to simulate herbaceous vegetation growth and soil water dynamics. The model runs on a daily time step and is a scale compatible with coarse resolution satellite remote sensing. STEP has been previously validated in two regions of the Sahel, namely the Ferlo (Senegal) and the Gourma (Mali) with field data acquired during the period 1976–1992 (Frison et al., 1998). Moreover, structural parameters such as vegetation cover fraction Vc, leaf area index (LAI), and canopy height hc, which are essential parameters for coupling with physical models of reflectivity, are also stimulated. Combined with an appropriate reflectance model, STEP was able to simulate temporal profile of vegetation indices which have been successfully compared with real satellite data (Lo Seen et al., 1995). In the following work, the STEP model is used to simulate the vegetation mass production and the volumetric water content in the upper soil profile.

To estimate these parameters, STEP model used soil texture, climate data (daily rain and temperature) maximum vegetation mass at the end of the rainy season (September).

Vegetation mass production, soil moisture estimates from STEP and soil roughness (estimated from the dry season radar data) and radar data are used to calibrate RTM (Optimization Step, Fig. 3).

After calibration of the RTM, we used it to estimate soil moisture from C-band radar data, daily vegetation mass production and soil roughness (inversion step, Fig. 3). To do this, a backpropagation algorithm was associated with the RTM. This algorithm looks for the values of the three parameters for which the same value as the radar coefficient is obtained. In fact, the main constraint has always been that one could get several triplets allowing to have the same value as the radar coefficient.

To solve this problem we used the Dry Mater Productivity (DMP) derived from the VEGETATION-2 optical sensor on SPOT-5 satellite, to estimate vegetation mass. The roughness was calculated from dry season radar data since it is the only parameter that influences the radar signal during this period. In fact, during the dry season, plant production is almost non-existent on the dry soil and only the surface roughness influences the radar response. Knowing these two parameters, the retro-propagation algorithm seeks the soil moisture level allowing the Radiative Transfer Model to restore the same value as the radar coefficient (we named this step: inversed model).

Then, the inversion of the model permits to calculate the soil moisture from radar data using the vegetation mass data from the DMP. Fig. 3 presents a summary of the sequences of the use of these two models (STEP and RTM).

Spatial-temporal variability of the estimated soil moisture is discussed regarding geology maps of the zone.

One part of the radar data used was measured during the day and the other part at night. We found it necessary to take only night measurements to minimize the effects of sunshine on humidity.

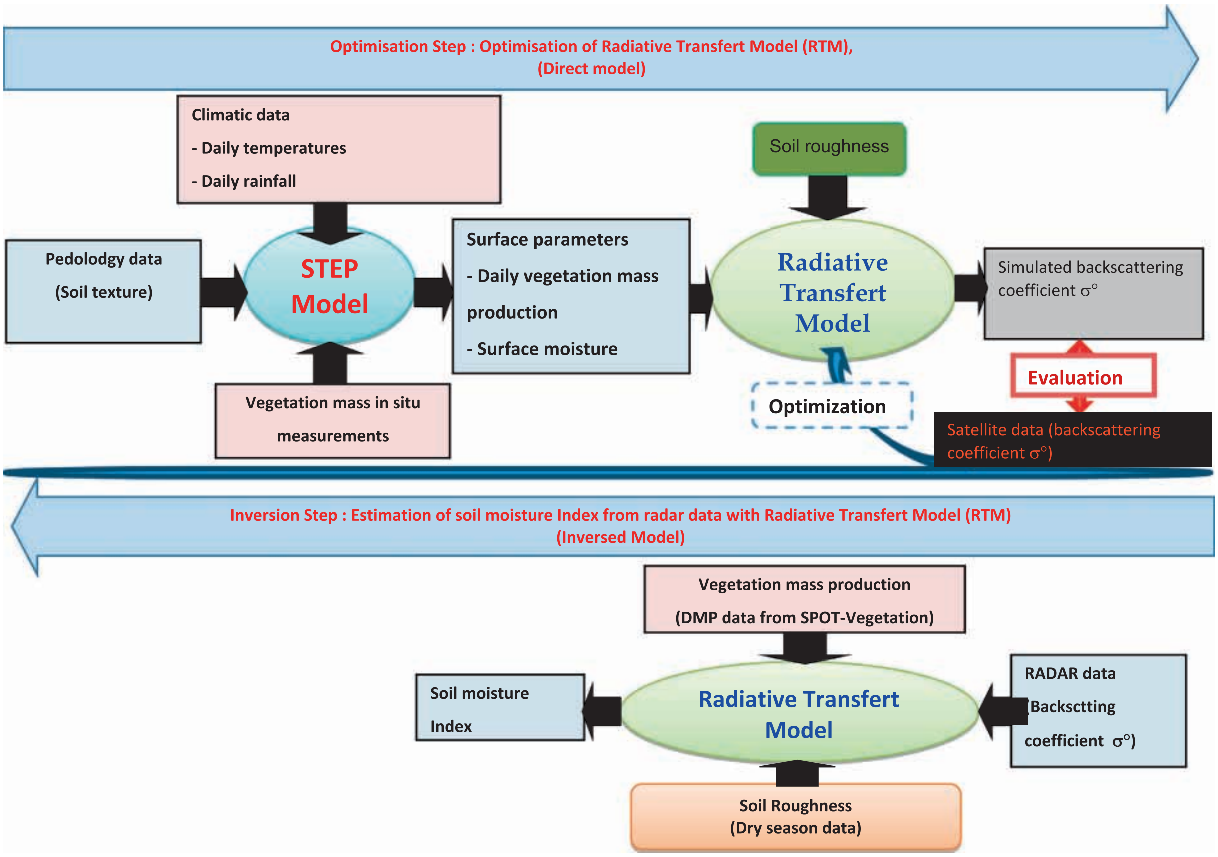

Fig. 3. Flow chart showing the various steps of estimating soil moisture.

To eliminate outliers, the following conditions were used in the model. This involves replacing the aberrant soil moisture Index values with a constant. We decided to replace all aberrant soil moisture Index by −3.33, a constant chosen arbitrary in order to facilitate cartography. These are pixels:

- having aberrant radar values (positives radar value in dB);
- having no radar value (not covered by the image);
- having a radar response high than −5.5 dB, so that the model fails to find for them a normal soil moisture value. Because in the Sahelian zone, with as much vegetation as possible, the maximum of signal is always lower than −5 dB (Faye et al., 2011; Frison and Mougin, 1996b; Frison et al., 1998; Jarlan et al., 2002, 2003; Zine et al., 2005). Then, the high value of signal is probably due to the contribution of other factors not related to vegetation, soil moisture and roughness. And it is difficult to interpret these other contributions with the model.

In the following, three soil moisture indices were calculated for each pixel for the four-years period 2008–2011:

- Maximum soil moisture index obtained during this period (Max SMI);
- Minimum soil moisture index obtained during this period (Min SMI);

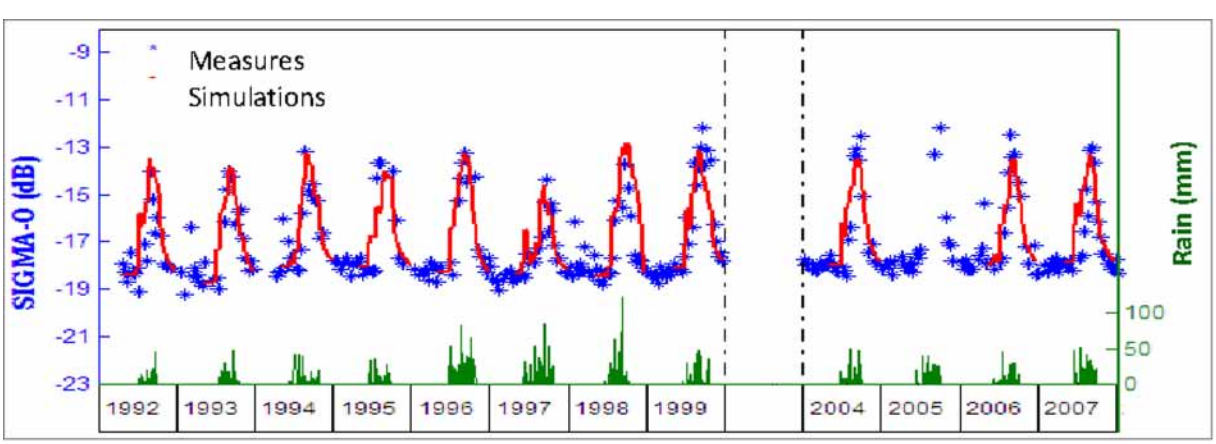

Fig. 4. Comparison of the measured and simulated radar signal.

- Average soil moisture index obtained during this period (Av SMI).

For this, we took the series of values (Soil moisture Index) obtained during this four-year period and calculated the maximum (Max SMI), the minimum (Min SMI) and mean (Av SMI).

For example: Av SMI of September = mean (all values obtained in September 2008 + all values obtained in September 2009 + all values obtained in September 2010 + all values obtained in September 2011).

For a better interpretation of the spatial dynamics observed for these indices, a first analysis was made to determine their sensitivity to the seasonal trend. Subsequently, a second analysis consisted in comparing the geological and geomorphological parameters with the indices. These two analyses permitted us to understand the spatial variability of these indices. Indeed, geology and geomorphology can influence the run-off/ infiltration.

Table 2
Annual amplitudes of measured and simulated coefficients.

Years	$\sigma°_{amp}$ measured (dB)	$\sigma°_{amp}$ simuled (dB)	Ecart relatif (%) (Measures – simulations)/simulations
1992	4,37	4,91	11,00%
1993	4,72	4,89	3,48%
1994	4,83	4,78	1,05%
1995	4,38	4,05	8,15%
1996	5,08	5,05	0,59%
1997	4,00	3,76	6,38%
1998	4,73	5,66	16,43%
1999	5,94	4,98	19,28%
2004	5,46	4,49	21,60%
2006	5,54	4,50	23,11%
2007	4,87	4,57	6,56%
Moyenne	5,21	4,69	10,69%

3. Results

3.1. Radar signal simulation

The first part of this work relates to the optimization of the Radiative Transfer Model using the long-term series of ESCAT data on board ERS-1 and ERS-2. Fig. 3 shows the comparison of the temporal signatures observed with the ESCAT scatterometer and the simulations by the direct model, after optimization (Fig. 4). Overall, good correlation was observed between the simulations and radar measurements, with an average error of 10% between the yearly amplitudes of σ° (Table 2). However, there were some small discrepancies between the amplitude of the measured signal and the simulated one, a consequence of the limit of the RTM. These results show that the model manages to restore the measured

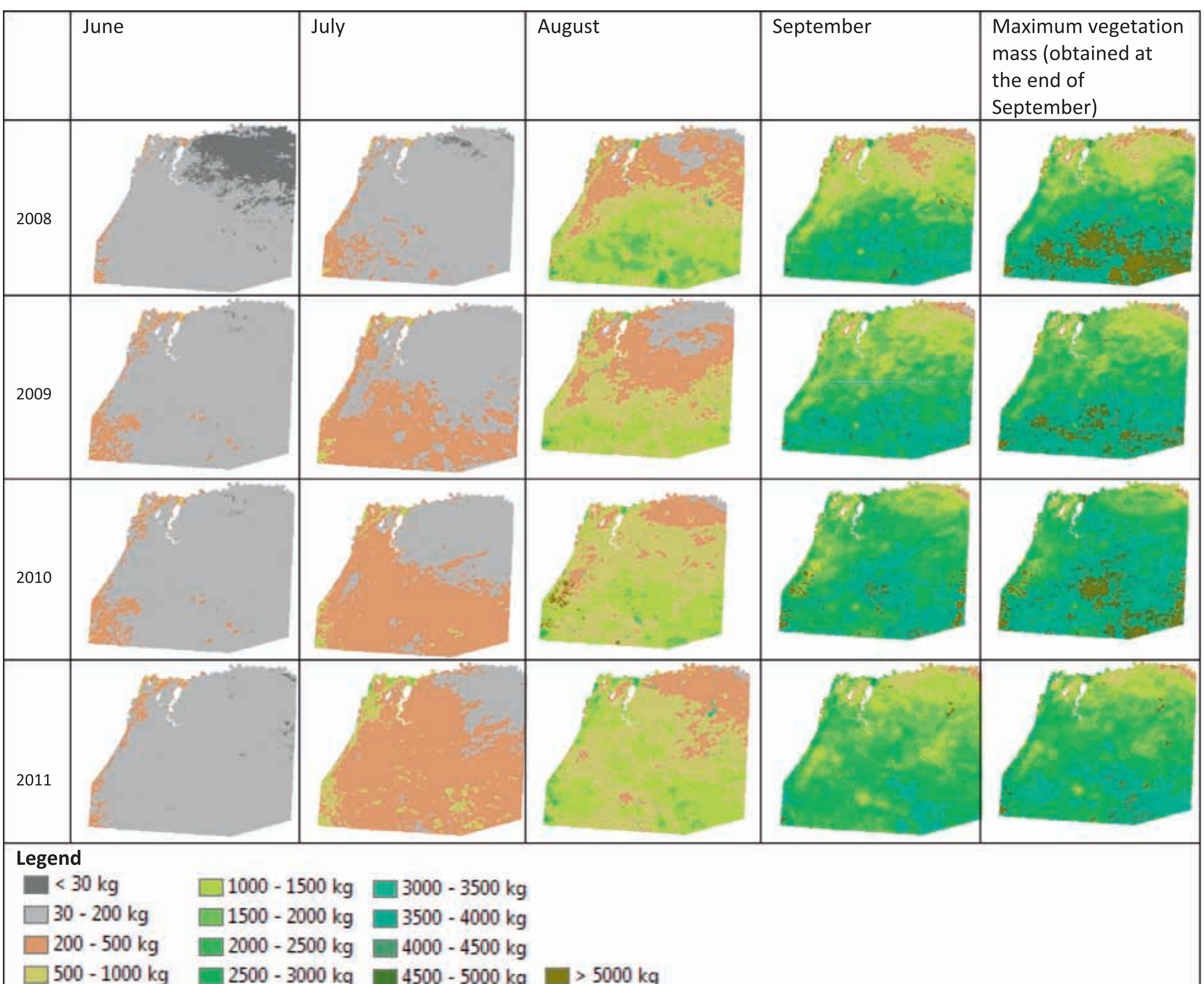

Fig. 5. Evolution of vegetation mass production estimated from SPTO-VGT DMP data over the study area during the growing season.

signal from the surface parameters (soil moisture, roughness and vegetation mass production) with 90% of precision.

3.2. Vegetation mass dynamic during the season

Fig. 5 shows the evolution of plant production calculated from DMP products. The month of June, corresponding to the beginning of the rainy season is marked by a very low plant production. This increases during the rainy season following a south-north gradient, before reaching its peak at the end of September.

3.3. Soil moisture dynamic

Given the low number of ASAR data covering the entire area, a monthly average of all survey years was made (e.g., June humidity is the average of moisture data for June of 2008, 2009, 2010 and 2011). We normalized the soil moisture values between 0 to 1, with 0 corresponding to completely dry soil and 1 a saturated soil. As the plant production, Fig. 6 show that soil moisture increases during the rainy season following a south-north gradient between June to September and decreases during October.

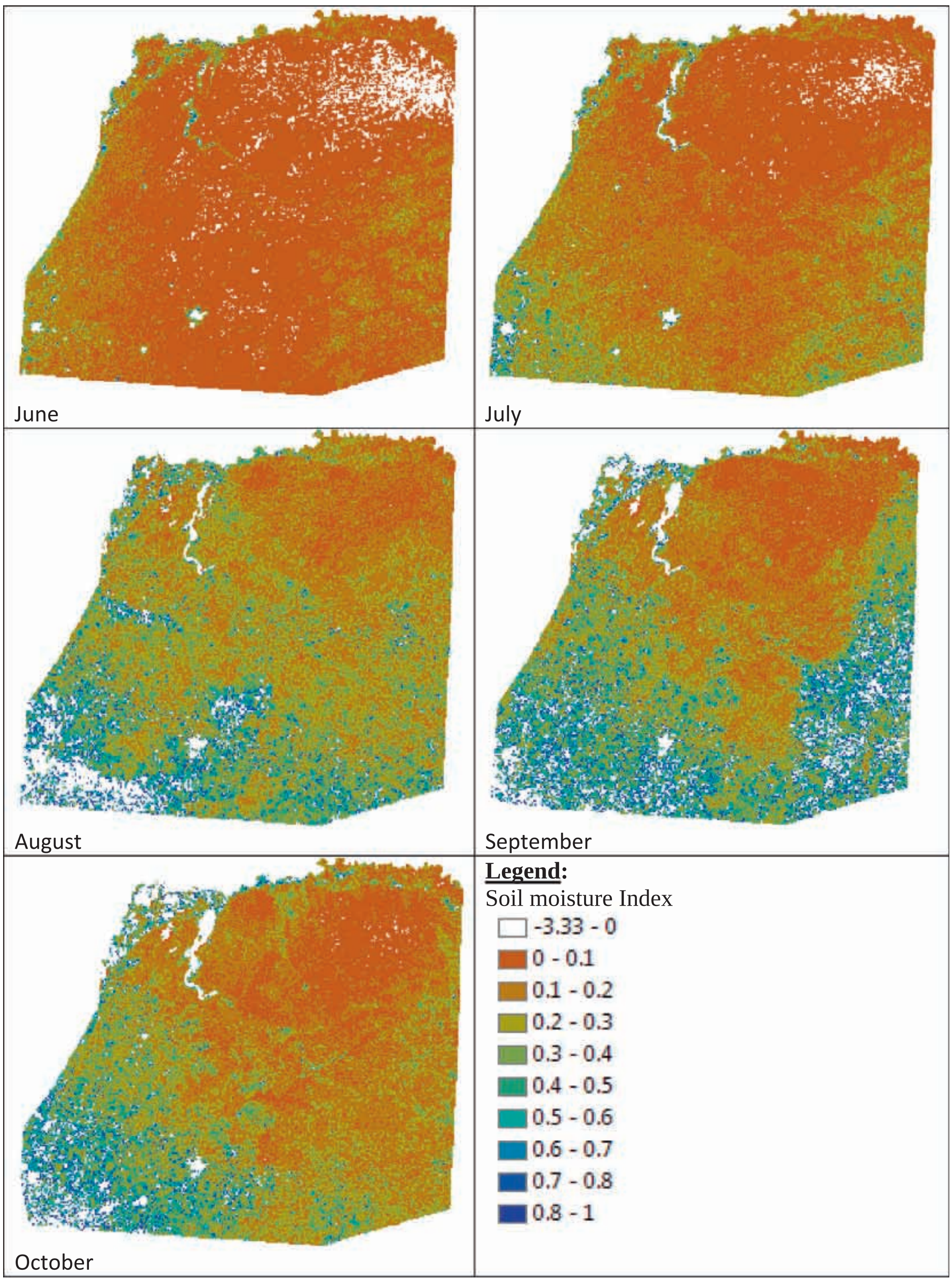

Fig. 6. Map of soil moistures estimated from radar data.

3.4. Analyze of soil moisture index

3.4.1. Maximum of soil moisture index

There is a strong north-south gradient of maximum soil moisture (Fig. 7a) showing strong correlation with the rainfall gradient. This high correlation results from the fact that soil moisture is often maximal just after it rains. The strong north-south gradient of rainfall in this area conditioned the spatial variability of the maximum moisture content. This limits the possibilities of confronting this indicator with the soil parameters.

3.4.2. Minimum of soil moisture index

Contrary to the maximum, the minimum soil moisture is not influenced by the rainfall gradient (Fig. 7b). Low values are observed in the central zone and especially in the north of the study area. The high values are encountered in the southeast of the study area but also and especially along the coast, with an extension towards the south. Such variability can be the result of several factors, notably soil characteristics.

Fig. 7b shows that the spatial extent of the minimum moisture content of the soil follows the geological contours in the south-eastern part of the study area where limestone sands with limestone outcrops, marls and kaolinic clays are present. Though to a lesser extent, this situation is also visible along the coastline and on the south-western part where alluvial and beach sands are encountered. However, in the central zone, there is no clear relationship between the spatial variation of the minimum soil moisture Index and the geological contours. The reason is that sand

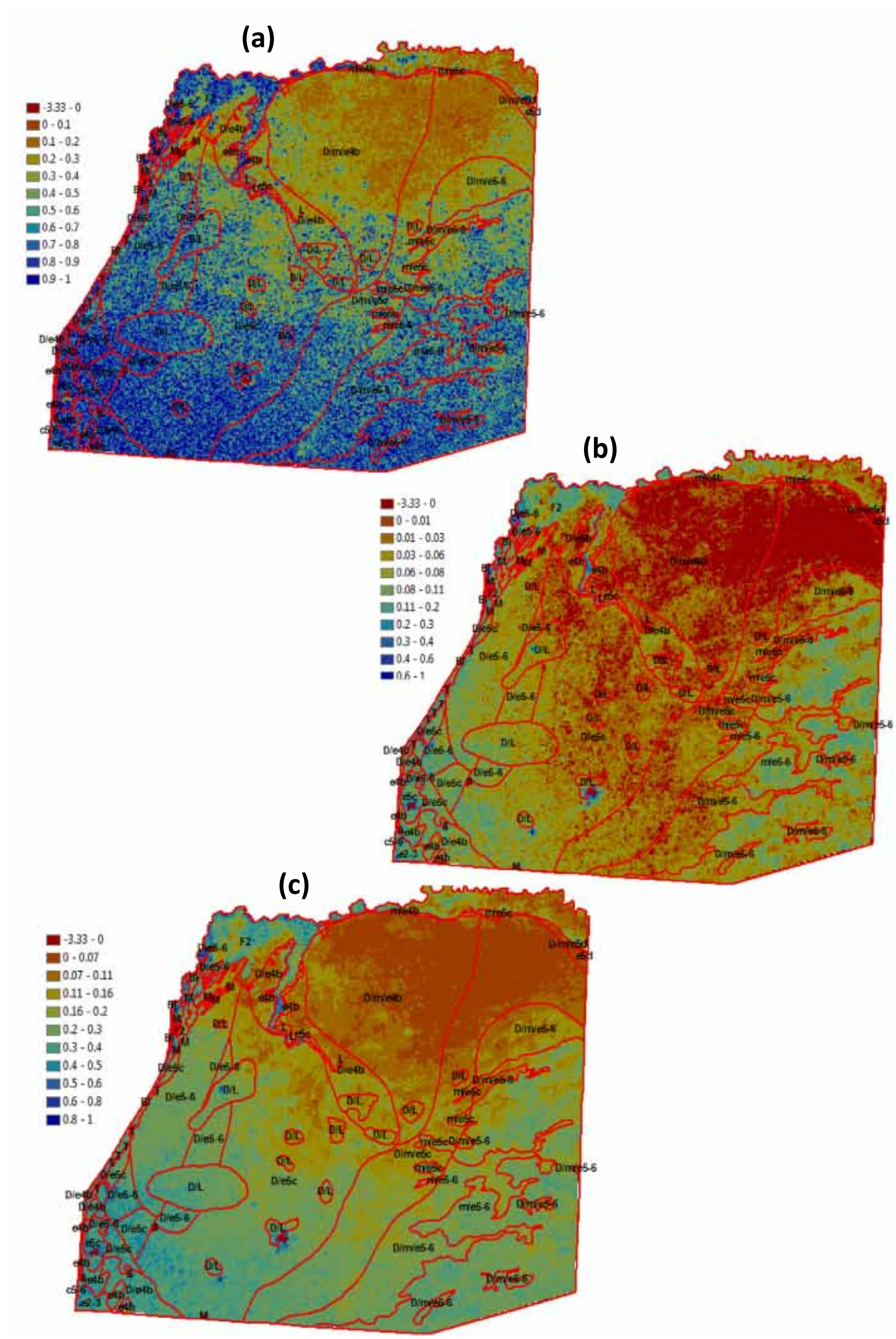

Fig. 7. Soil moisture Index dynamic.

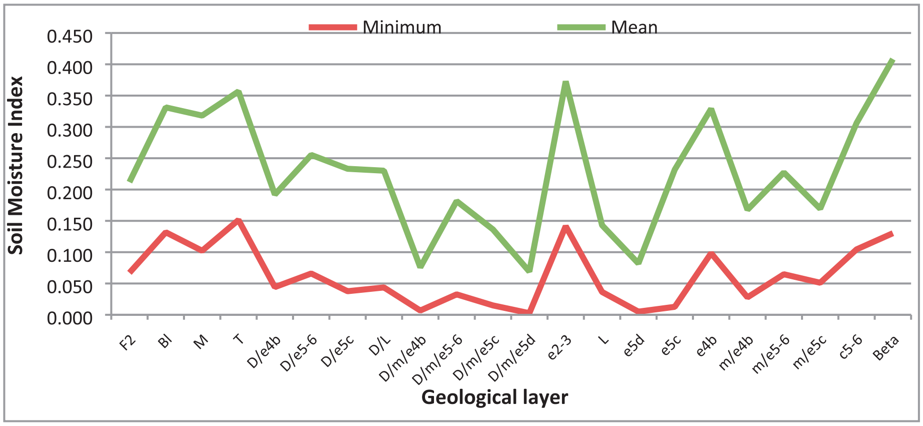

Fig. 8. Variation of soil moisture index (minimum and average) according to the geological layers.

dunes in the center have a high infiltration rate, which causes the very quick disappearance of soil moisture, leaving a dry soil in place. On the contrary, loamy sands with outcrops of limestone, marls and kaolinic clay have a high-water retention capacity, thus greater persistence of soil moisture after the rain. This is more the reason that this area hosts many temporary pools that retain water even during much of the dry season.

3.4.3. Mean of soil moisture index

High spatial variability in soil moisture values is observed with high values in the southwest (Fig. 7c). The south-eastern part also has fairly high values, contrary to the north-central region where humidity averages are very low. Like minimum humidity, this strong spatial dynamic may result from the characteristics of the superficial geological layers of the zone.

Furthermore, as in the case of the minimum humidity, a strong correlation between the dynamics of the average soil moisture and the geological contours in the southeast and on the coast, is observed in Fig. 7c. It is also found that in the central zone, characterized by dune sands, the spatial variability of mean humidity is related to the lithology. Average soil moisture depends on geology in some places although the dune sands have a high infiltration rate.

The low variability of the minimum moisture content for dune sand (layers beginning with the letter D in Fig. 8 and Table 1) observed confirms the observations in Fig. 7 where there was no relationship between the minimum moisture and geological contours. For the other layers, we notice strong dynamic materializing the correlation between the geology and minimum humidity.

The saw tooth variation of the mean moisture shows that this index is strongly dependent on geology.

4. Discussion

The seasonal variability of the radar signal amplitude indicates the dynamic character of annual crop production in the Sahel. However, in this area, plant production is mainly dependent on rainfall, which is very variable. The seasons are characterized by a north-south gradient with a FIT moving from south to north. This results in very low or no humidity at all in the northern half of the study area at the beginning of the rainy season (i.e., June). It then increases slightly in July, particularly in the southern half of the zone where a high degree of humidity is observed in the extreme southwest. This trend continues during the months of August and September following a north-south gradient. There is a high humidity in September in the south-eastern and south-western parts of the zone, with some aberrant values due to the the saturation of the signal. This saturation can result from two things:

- a soil saturated in places, causing a very high signal and thus causing a misinterpretation by the Radiative Transfer Model;
- a strong roughness induced by agriculture exploitations in this part during the rainy season. This part of the study area is an agriculture zone, so we assumed that the roughness is constant throughout the year.

The strong gradient of the maximum humidity observed is conditioned by the spatial variability of the rainfall. This is quite normal, maximum moisture is observed in the south. As for both the mean and minimum humidity, there is a strong correlation with the nature of the geological formations. This situation is explained by the fact that the ground's water retention capacity is subject to its geology.

5. Conclusion and perspectives

This work was based on a combination of radar and optical data for an estimation of soil moisture and yielded promising results. In fact, due to the sensitivity of the radar signal to plant production, roughness and soil moisture, it has always been difficult to determine from the radar signal the contribution of each of these parameters to deduce their respective values. The technique of calculating vegetation mass from optical data, estimating roughness from dry season radar data and then estimating their contribution and deducing the value of soil moisture is a major step forward. Nevertheless, there are many soil moisture values classified as aberrant, resulting from a misinterpretation of the signal by the Radiative Transfer Model. Using data with a good time repeat might help filter these values.

Conflicts of interest

None.

References

Aubert, M., Baghdadi, N., Zribi, M., Douaoui, A., Loumagne, C., Baup, F., El Hajj, M., Garrigues, S., 2011. Analysis of TerraSAR-X data sensitivity to bare soil moisture, roughness, composition and soil crust. Remote Sens. Environ. 2011 (115), 1801–1810.

Anguela, T.P., Zribi, M., Baghdadi, N., Loumagne, C., 2010. Analysis of local variation of soil surface parameters with TerraSAR-X radar data over bare agricultural fields. IEEE Trans. Geosci. Remote Sens. 2010 (48), 874–881.

Baghdadi, N., Zribi, M., Loumagne, C., Ansart, P., Anguela, T.P., 2008. Analysis of TerraSAR-X data and their sensitivity to soil surface parameters over bare agricultural fields. Remote Sens. Environ. 2008 (112), 4370–4379.
Baghdadi, N., Cresson, R., El Hajj, M., Ludwig, R., La Jeunesse, I., 2012. Estimation of soil parameters over bare agriculture areas from C-band polarimetric SAR data using neural networks. Hydrology and earth system sciences. Eur. Geosci. Union 16, 1607–1621.
Baup, F., Mougin, E., De Rosnay, P., Timouk, F., Chênerie, I., 2007. Surface soil moisture estimation over the AMMA Sahelian site in Mali using ENVISAT/ASAR data. Remote Sens. Environ. 109 (2007), 473–481.
Bégué, A., 2002. Télédétection et production végétale. Habilitation à Diriger des Recherches. Université Pierre et Marie Curie, France, p. 112.
Bernard, R., Vauclim, M., Vidal-Madjoar, D., 1981. Possible use of active microwave remote Sensing data for prediction of regional evaporation by numerical simulation of soil water movement in the unsaturated zone. Water Resour. Res 17 (6), 1603–1610.
Bradley, G.-A., Ulaby, F.-T., 1981. Aircraft radar response to soil moisture. Remote Sens. Environ. 11, 419–438.
Bruckler, L., Wittono, H., Stengel, P., 1988. Near surface moisture estimation from microwave measurements. Remote Sens. Environ. 26, 101–121.
Castaldi, F., Casa, R., Castrignanò, A., Pascucci, S., Palombo, A., Pignatti, S., 2014. Estimation of soil properties at the field scale from satellite data: a comparison between spatial and non-spatial techniques. Eur. J. Soil Sci. 2014 (65), 842–851.
Diouf, A., Sall, M., Wele, A., Drame, M., 1998. Méthode d'échantillonnage de la Production Primaire sur le Terrain. CSE, p. 9.
M.-C. Dobson F.-T. Ulaby 1986 Active microwave soil moisture research IEEE Trans. Geosci. Remote Sens. GE-24 1 23 36
Dubois, P.-C., Van Zyl, J., Engman, T., 1995. Measuring soil moisture with imaging radars. IEEE Trans. Geosci. Remote Sens. 33, 877–895.
Faye, G., Frison, P.-L., Wade, S., Ndione, J.-A., Beye, A.-C., Rudant, J.-P., 2011. Etude de la saisonnalité des mesures des diffusiomètres SCAT: apport au suivi de la végétation au Sahel, cas du Ferlo au Sénégal. Télédétection 10 (1), 23–31.
Frison, P.-L., Mougin, E., 1996a. Use of the ERS-1 Wind scatterometer data over land surfaces. IEEE Trans. Geosci. Remote Sens. 34 (2), 550–560.
Frison, P.L., Mougin, E., 1996b. Monitoring global vegetation dynamics with ERS-1 wind-scatterometer data. Int. J. Remote Sens. 17, 3201–3218.
Frison, P.-L., Mougin, E., Hiernaux, P., 1998. Observations and interpretation of seasonal ERS-1 wind scatterometer data over Northern Sahel (Mali). Remote Sens. Environ. 693, 233–242.
Gorrab, A., Zribi, M., Baghdadi, N., Mougenot, B., Lili Chabaane, Z., 2015. Potential of X-Band TerraSAR-X and COSMO-SkyMed SAR Data for the assessment of physical soil parameters. Remote Sens. 2015 (7), 747–766.
Jarlan, L., Mougin, E., Frison, P.-L., Mazzega, P., Hiernaux, P., 2002. Analysis of ERS wind scatterometter time series over Sahel (Mali). Remote Sens. Environ. 81, 404–415.
Jarlan, L., Mazzega, P., Mougin, E., Lavenu, F., Marty, G., Frison, P.-L., 2003. Mapping of Sahelian vegetation parameters from ERS scatterometer data with an evolution strategies algorithm. Remote Sens. Environ. 87, 72–84.
Karam, M.-A., Fung, A.-K., Lang, R.-H., Chauhan, N.-S., 1992. Microwave scattering model for layered vegetation. IEEE Trans. Geosci. Remote Sens. 30, 767–784.
Kumar, M., Monteith, J.L., 1981. Remote Sensing of Crop Growth. Plants and the daylight spectrum, pp. 133–144.
Le Toan, T., Paulsader, M., Flouza, t G., Fluhr, A., 1981. Soil moisture content and microwave backscatter in the 1.5-9 GHZ region. Invited paper, Int. Geosci. Remote Sensing. Symp., Washington, DC, juin.
Lo Seen, D., Mougin, E., Rambal, S., Gaston, A., Hiernaux, P., 1995. A regional Sahelian grassland model to be coupled with multispectral satellite data. II. Towards the control of its simulations by remotely sensed indices. Remote Sens. Environ. 52, 194–206.
Magagi, R.D., Kerr, Y.H., 1997. Retrieval of soil moisture and vegetation characteristics by use of ERS-1 wind scatterometer over arid and semiarid areas. J. Hydrol. 188–189, 361–384.
Molin, J.P., Faulin, G.D.C., 2013. Spatial and temporal variability of soil electrical conductivity related to soil moisture. Sci. Agric. 2013 (70), 1–5.
Mougin, E., Lo Seen, D., Rambal, S., Gaston, A., Hiernaux, P., 1995. A regional sahelian grouland model to be coupled with multispectral data. Description et validation. Remote Sens. Environ. 52, 181–193.
Naeimi, V., Scipal, K., Bartalis, Z., Hasenauer, S., Wagner, W., 2009. An improved soil moisture retrieval algorithm for ERS and METOP scatterometer observations. IEEE Trans. Geosci. Remote Sens. 47 (7), 1999–2013. https://doi.org/10.1109/TGRS.20082011617.
Pandey, V., Pandey, P.K., 2010. Spatial and temporal variability of soil moisture. Int. J. Geosci. 2010 (1), 87–98.
Pellarin, T., Calvet, J.C., Wagner, W., 2006. Evaluation of ERS scatterometer soil moisture products over a half-degree region in southwestern France. Geophys. Res. Lett. 33 (17), L17401.
PNAT, 1986, Cartographie et télédétection des ressources de la république du Sénégal. Etude de la géologie, de l'hydrologie, des sols, de la végétation et des potentiels d'utilisation des sols. SDSU-RSI-86-01, p. 653.
Rahman, M.M., Moran, M.S., Thoma, D.P., Bryant, R., Holifield Collins, C.D., Jackson, T., Tischler, M., 2008. Mapping surface roughness and soil moisture using multi-angle radar imagery without ancillary data. Remote Sens. Environ. 112 (2), 391–402.
Thoma, D.P., Moran, M.S., Bryant, R., Rahman, M.M., Holifield Collins, C.D., Keefer, T. O., Noriega, R., Osman, I., Skrivin, S.M., Tischler, M.A., 2008. Appropriate scale of soil moisture retrieval from high resolution radar imagery for bare and minimally vegetated soils. Remote Sens. Environ. 2008 (112), 403–414.
Ulaby, F.-T., Batlivala, P.-P., Dobson, M.C., 1978. Microwave backscatter dependence on surface roughness, soil moisture and soil texture, Part 1, Bare soil. IEEE Trans. Geosci. Remote Sens. 16, 286–295.
Varlet-Grancher, C., Bonhomme, R., Chartier, M., Artis, P., 1982. Efficience de la conversion de l'énergie solaire par un couvert végétal. Acta Oecologica. Oecologia Plantarum 3, 3–26.
Wagner, W., Lemoine, G., Rott, H., 1999. A method for estimating soil moisturefrom ERS scatterometer and soil data. Remote Sens. Environ. 70 (2), 191–207.
Wagner, W., Scipal, K., 2000. Largescale Soil moisture mapping in western Africa using the ERS Scatterometer. IEEE Trans. Geosci. Remote Sens. 38, 1777–1782.
Woodhouse, I.H., Hoekman, D.H., 2000. Determining land surface parameters from the ERS-1 wind scatterometer. IEEE Trans. Geosci. Remote Sens. 38, 126–140.
Zine, S., Jarlan, L., Frison, P.-L., Mougin, E., Hiernaux, P., Rudant, J.-P., 2005. Land surface parameter with ERS scatterometer data over the Sahel: a comparison between agro-pastoral and pastoral areas. Remote Sens. Environ. 693, 438–452.
Zribi, M., Dechambre, M., 2002. A new empirical model to retrieve soil moisture and roughness from C-band radar data. Remote Sens. Environ. 84, 42–52.
Zribi, M., Chahbi, A., Lili Chabaane, Z., Duchemin, B., Baghdadi, N., Amri, R., Chehbouni, A., 2011. Soil surface moisture estimation over a semi-arid region using ENVISAT ASAR radar data for soil evaporation evaluation. Hydrol. Earth Syst. Sci. 2011 (15), 345–358.
Zribi, M., Gorrab, A., Baghdadi, N., 2014. A new soil roughness parameter for the modelling of radar backscattering over bare soil. Remote Sens. Environ. 2014 (152), 62–73.